J Mater Sci (2011) 46:2467–2473
DOI 10.1007/s10853-010-5093-0

Intermetallic phase formation in diffusion-bonded Cu/Al laminates

Yajie Guo · Guiwu Liu · Haiyun Jin · Zhongqi Shi · Guanjun Qiao

Received: 29 July 2010 / Accepted: 16 November 2010 / Published online: 1 December 2010

Abstract Intermetallic phase formation in diffusion-bonded Cu/Al laminates prepared by plasma activated sintering (PAS) was investigated in the temperature range 673–773 K for 10–30 min. Three intermetallic phases, Al_4Cu_9, AlCu, and Al_2Cu, were identified in all the samples. The formation of Al_2Cu as the first phase was rationalized on the basis of the effective heat of formation (EHF) model. The thermodynamic driving force for the preferential appearance of Al_4Cu_9 at the α-Cu(Al)/Al_2Cu interface was evaluated. The time and temperature dependences of the growth of the three intermetallic layers were determined, and their apparent activation energies were calculated. The growth kinetic of the layers conformed to the parabolic law, implying that the intermetallic phase formation was volume diffusion-controlled in the temperature range. The apparent activation energies calculated for the growth of the total intermetallic layer, Al_4Cu_9, AlCu, and Al_2Cu layers were about 80.8, 89.8, 84.6, and 71.1 kJ/mol, respectively.

Y. Guo (✉) · G. Liu · Z. Shi · G. Qiao (✉)
State Key Laboratory for Mechanical Behavior of Materials, School of Materials Science and Engineering, Xi'an Jiaotong University, 28 Xianning West Road, Xi'an, Shaanxi Province 710049, People's Republic of China
e-mail: yajie.guo@gmail.com

G. Qiao
e-mail: gjqiao@mail.xjtu.edu.cn

G. Liu
MOE Key Laboratory for Strength and Vibration, Xi'an Jiaotong University, Xi'an 710049, China

H. Jin
School of Electrical Engineering, Xi'an Jiaotong University, Xi'an 710049, China

Introduction

Intermetallic phase formation during solid-state diffusion between binary dissimilar metals is an important phenomenon in many areas including welded and bonded components [1], composites [2], thin-film electronic devices and metallization [3, 4]. Due to the limited solid-state solubility of Cu–Al system, few intermetallic phases may form when the two metals are brought into contact [5, 6]. These brittle intermetallic phases have significant influence on the manufacturability, mechanical properties, and reliability of the Cu–Al structures. Therefore, to understand the intermetallic phase formation at the Cu/Al interface is of both scientific and technological importance.

Previous study showed that different intermetallic phases may form at the Cu/Al solid-state diffusion interface in terms of the different methods and conditions used in the experiments. Funamizu and Watanabe [6] studied the multiphase diffusion between Cu and Al using bulk couples at 673–808 K for a maximum duration of 100 h. They reported the formation of all the possible five equilibrium phases predicted by the Cu–Al phase diagram, i.e., Al_4Cu_9, Al_2Cu_3, Al_3Cu_4, AlCu, and Al_2Cu. However, Hannech et al. [7] found that the Al_4Cu_9 was absent in the bulk couples annealed at 698 K for 25–225 h. Moreover, in the case of the hot roll bonded Cu–Al laminates, the formation of intermetallic phases was not only dependent on the temperature [8], but also on the time as well [2]. In addition, Abbasi et al. [9] investigated the cold roll bonded Al/Cu bimetal annealed at 523 K for 1–1000 h and detected $AlCu_3$, Al_3Cu_4, AlCu, and Al_2Cu at the interface. However, in the friction welded Cu/Al bimetallic joints annealed at 573–773 K for 1–36 h, Lee et al. [10] only found two intermetallic phases (AlCu and Al_2Cu) at the interface. As stated above, several variables, such as the

processing condition, annealing temperature and time, can affect the formation of the intermetallic phases at the interface. However, there is still some scientific confusion about the reactive phase formation between Cu and Al that need to be clarified.

This study focuses on the intermetallic phase formation at Cu/Al interface during diffusion bonding in the temperature range 673–773 K. The interfacial morphology and intermetallic phases formed are examined. The sequence of the phase formation is rationalized using the effective heat of formation (EHF) model and thermodynamic analysis. The growth kinetic of the intermetallic layers is determined simultaneously.

Experimental

Commercially available foils of Cu (99.9 wt%) and Al (99.7 wt%) were used with an initial thickness of 200 μm. Both the Cu and Al foils were machined into disks of Ø 20 mm by a spark cutter. To improve the interfacial bonding between Cu and Al, the Cu and Al disks were etched in 15% HCl and 10% NaOH solutions, respectively, and then ultrasonically cleaned in alcohol, flushed in water, and dried in turn. Five Cu disks and four Al disks were alternately stacked into a graphite die, subsequently processed by PAS (Ed-PAS III, Elenix Ltd., Japan) at 673 K, 723 K, and 773 K (heating rate: 200 K/min) for 10–30 min with the intervals of 5 min under an uniaxial pressure of 10 MPa in argon atmosphere (0.12 MPa). The PAS is a recent innovation pioneered by Sodick Co., Ltd. in Japan. The combination of pulsed direct current, continuous direct current, and pressure application enables the PAS to accomplish a rapid sintering. A detailed description of the PAS process was given elsewhere [11].To accurately control the temperature, a thermocouple was placed to contact directly with the samples, through a through-hole made in the graphite die wall.

The diffusion-bonded couples were sectioned along the direction perpendicular to the bond interface with a low-speed diamond saw, mounted, and prepared by standard metallographic technique. Microstructural observation was performed via scanning electron microscope (SEM, JSM-7000F, JEOL, Japan or VEGAII XMU, Tescan, Czech) and transmission electron microscope (TEM, JEOL-2000EX II). For the TEM observations, a cross-sectional specimen was cut into 300 μm thick and then ground to 40 μm. The final thinning was made by ion milling. The TEM analysis was performed under an accelerated voltage of 200 kV. The intermetallic phases formed at the interface were identified by energy dispersive X-ray spectrometer (EDS, Model Oxford INCA, British) and X-ray diffractometer (XRD, Model X'Pert PRO, PANalytical, Ltd., Holland). To determine the growth kinetic of the intermetallic phases, the thicknesses of the total intermetallic layer and each individual layer were examined from SEM micrographs of the cross-sections. An average thickness was obtained from 20 individual measurements.

Results and discussion

Interface microstructure and reaction product identification

The PAS-processed laminates exhibited good bonding between Cu and Al foils, as shown in Fig. 1. Typical back–scatter–Electron (BSE) micrographs of the multi-laminated samples annealed 10 min at different temperatures are shown in Fig. 2. Three distinct reaction layers, parallel to the interface, can be observed in the interfacial zone. No cracks and voids existed in the interfacial reaction layers. The thickness of the reaction layers increased remarkably with the annealing temperature and/or time increasing (Fig. 2). The EDS analysis elucidated that the composition of the three layers, arrayed in sequence from Cu to Al, corresponded to Al_4Cu_9, AlCu, and Al_2Cu phases, respectively. These phases were further determined by XRD (on the as-peeled samples) and TEM analyses (Figs. 3, 4). Further experiments showed that the identical intermetallic phases, i.e., Al_4Cu_9, AlCu, and Al_2Cu, were found in the temperature range 673–773 K for 10–30 min. The intermetallic phases formed here were consistent with the literatures [12, 13]. Note that Al_2Cu_3 and Al_3Cu_4 were not detected in this study, probably due to their low growth rate.

Formation of interfacial phases

The Cu–Al phase diagram indicates five equilibrium phases, Al_4Cu_9, Al_2Cu_3, Al_3Cu_4, AlCu, and Al_2Cu, in the

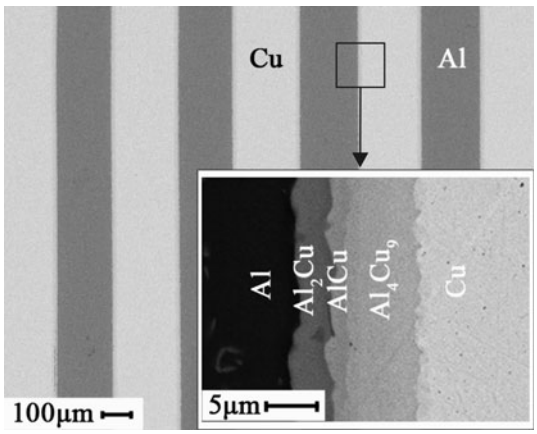

Fig. 1 A typical BSE image of diffusion-bonded Cu–Al laminates conducted at 723 K for 30 min

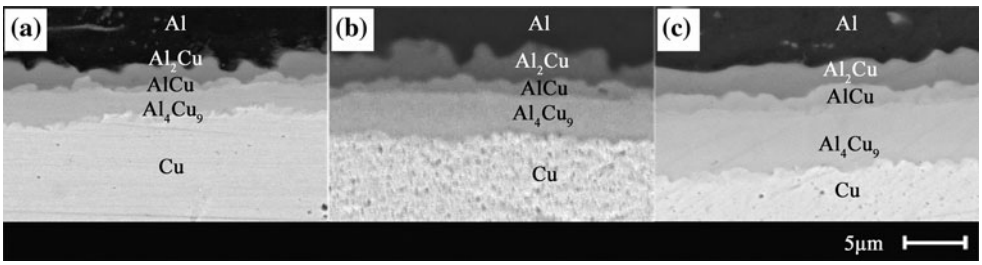

Fig. 2 BSE micrographs of the interfacial zone annealed for 10 min at **a** 673 K, **b** 723 K, and **c** 773 K

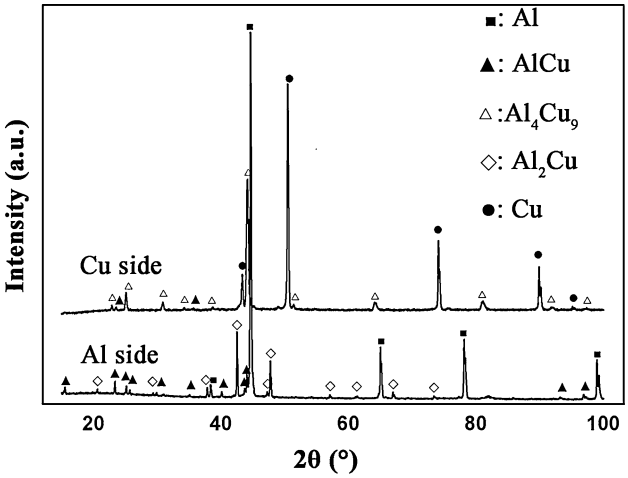

Fig. 3 XRD patterns taken from an as-peeled sample

temperature range 673–773 K, of which only Al_4Cu_9, AlCu, and Al_2Cu were found in this study. Among these phases, Al_4Cu_9 has the most negative free energy of formation [14]. Therefore, thermodynamically it is expected to form first at the Cu–Al interface in the solid-state diffusion process. However, this does not agree with the experimental observation that Al_2Cu was the first phase appeared between Cu and Al [5, 15, 16]. Clearly, the kinetic influences must be taken into account in the theoretical models for a correct prediction. In the case of the Cu–Al system, saturated solid solutions of α-Cu(Al) and β-Al(Cu) formed on the each side due to interdiffusion. Note that the solubility limit of Al in Cu is 19.7 at% in the temperature range 673–773 K, while the maximum solubility limit of Cu in Al in the same temperature range is only 2.48 at% [14]. Since the solubility limit of Cu in Al is an order of magnitude less than that of Al in Cu, the Al(Cu) solid solution would be expected to saturate first, resulting in the nucleation of Al_2Cu, as experimentally observed by previous study [3].

Among a number of models for predicting the formation of first phase in a binary system, the effective heat of formation (EHF) model developed by Pretorius et al.

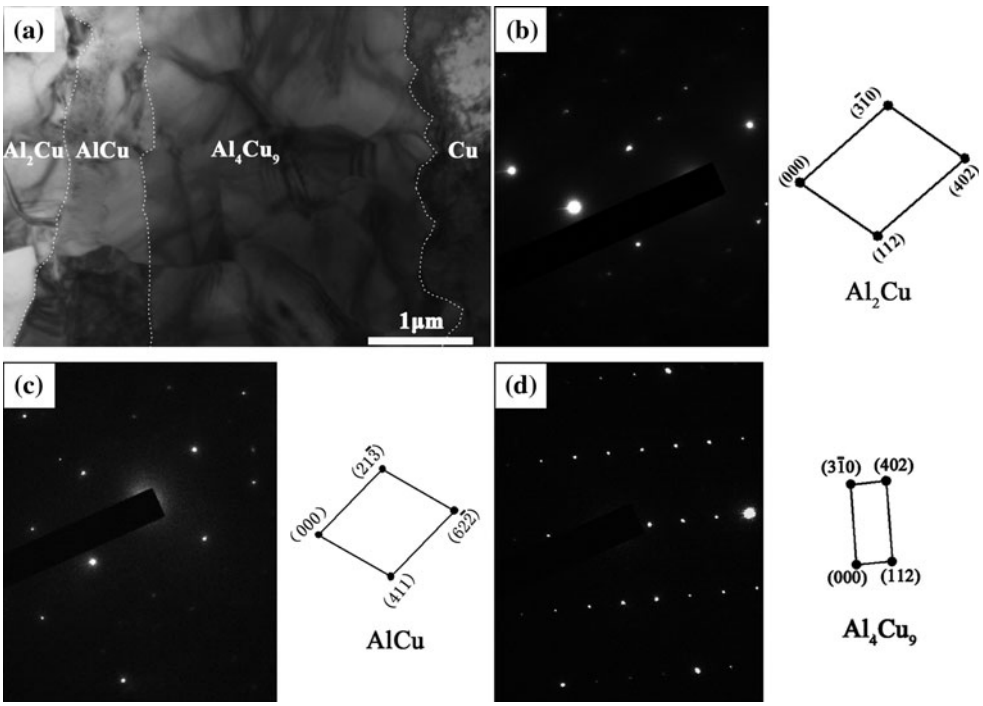

Fig. 4 **a** Bright-field TEM image of interface and diffraction patterns and schematic index diagram of **b** Al_2Cu, **c** AlCu, and **d** Al_4Cu_9 for laminates conducted at 673 K for 20 min

Table 1 The composition and corresponding effective heat of formation of the Cu–Al intermetallic phases

Intermetallic phase	Cu concentration (at%)	Limiting element	ΔH° [14] (kJ/mol)	$\Delta H'$ (kJ/mol)
Al_2Cu	33	Cu	–13.05	–6.76
AlCu	51	Cu	–19.92	–6.68
Al_3Cu_4	55.5	Cu	–20.40	–6.29
Al_2Cu_3	60.5	Cu	–20.67	–5.84
Al_4Cu_9	66	Cu	–21.69	–5.61

[17, 18] was succeeded in predicting the formation of first phase in many binary systems [19, 20]. The EHF model combined the thermodynamic data with the concentrations of the reaction species at the growth interface. Based on this model, the EHF, $\Delta H'$, is defined as [17]:

$$\Delta H' = \Delta H^\circ \times \frac{C_e}{C_1} \tag{1}$$

where ΔH° is the standard heat of formation. C_e is the effective concentration of the limiting element (The element which will be used up first during the formation of one phase) at the interface, taken as the composition of the limiting element at the lowest eutectic temperature. C_1 is the concentration of the limiting element in the compound.

On the basis of this model, the values of $\Delta H'$ were calculated for all the five intermetallic phases in the experimental temperature range and are listed in Table 1 along with the values of ΔH°. It can be seen that Al_2Cu has the maximum negative EHF ($\Delta H'$) and hence was expected to form first in the diffusion zone. This result illustrated the first nucleation of Al_2Cu in view of thermodynamics combined with kinetic theory, which has not ever been considered in spite of a lot of previous study on this system.

Previous study [5, 15, 21] suggested that Al_4Cu_9 would be the next phase followed Al_2Cu to appear in the diffusion zone, but the reason was not still interrupted clearly. The possible reason for the preference can be explained considering the thermodynamic drive force at the α-Cu(Al)/Al_2Cu interface.

The free energy for a solid solution phase in a binary system A–B can be represented mathematically as follows [22]:

$$G^S = C_A G_A + C_B G_B + \Delta H^S_{mix} + T\Delta S^S_{mix} \tag{2}$$

where C_A and C_B are the mole fractions of A and B, respectively. G_A and G_B are the Gibbs free energy of the pure element A and B, respectively. ΔH^S_{mix} is the enthalpy change during intermixing, ΔS^S_{mix} $(= -R(C_{Al} \ln C_{Al} + C_{Cu} \ln C_{Cu}))$ is the entropy of intermixing. The enthalpy change of a solid solution phase can be determined by the semi-experimental Miedema's model [23–25]:

$$\Delta H^S_{mix} = \Delta H^C + \Delta H^E + \Delta H^S \tag{3}$$

where the three terms are the chemical, elastic, and structural contributions, respectively. The chemical term ΔH^C is calculated by:

$$\Delta H^C = C_A C_B \left(C^S_B \Delta H^{Sol}_{A \text{ in } B} + C^S_A \Delta H^{Sol}_{B \text{ in } A} \right) \tag{4}$$

where $\Delta H^{Sol}_{A \text{ in } B}$ is the solution enthalpy of A in B and can be calculated by the method proposed by Miedema et al. C^S_B is the degree to which A atoms are in contact with B atoms, and can be expressed as:

$$C^S_B = 1 - C^S_A = \frac{C_B V_B^{2/3}}{C_A V_A^{2/3} + C_B V_B^{2/3}} \tag{5}$$

where V_A and V_B are the mole volumes of A and B, respectively. The elastic term for a solid solution phase is expressed by:

$$\Delta H^E = C_A C_B \left(C_A \Delta H^e_{B \text{ in } A} + C_B \Delta H^e_{A \text{ in } B} \right) \tag{6}$$

where $\Delta H^e_{B \text{ in } A}$ is the elastic contribution to the heat of solution of B in A in the solid solution phase, and can be calculated by the method proposed by de Boer et al. [26]. The third term, ΔH^S, is different from zero only for transition metal-transition metal alloys [27]. For the Cu–Al solutions, Cu is a transition metal and Al a main group metal, so the structure contribution $\Delta H^S = 0$.

Based on the equations described above, the Gibbs free energy-composition diagrams at 773 K were plotted for α-Cu(Al) solid solution, Al_4Cu_9, Al_2Cu_3, Al_3Cu_4, AlCu, and Al_2Cu, as shown in Fig. 5. The values of the Gibbs free energy G_A and G_B were taken from the literature [28]. The parameter values for calculations of ΔH^S_{mix} were taken from the literature [29]. Assuming local equilibrium between α-Cu solid solution and Al_2Cu, we can draw a

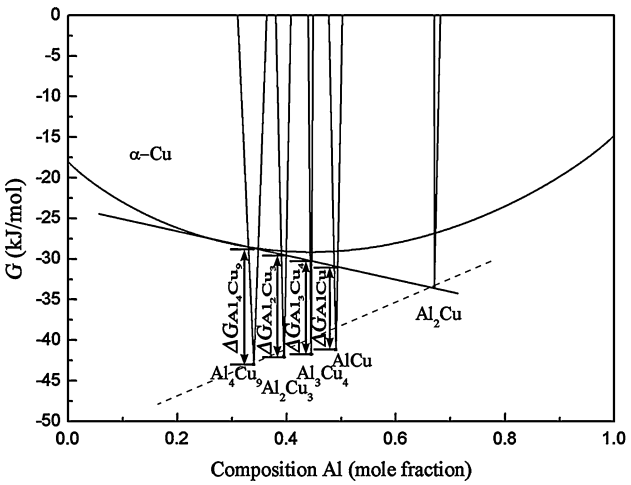

Fig. 5 Free energy (G) versus composition (C_{Al}) plot of the Cu–Al system at 773 K

common tangent between the two curves. Clearly, the driving force for formation of Al_4Cu_9 was more negative than those for the other phases at 773 K, resulting in the preferential formation of Al_4Cu_9 at the α-Cu/Al_2Cu interface.

Similarly, for the local equilibrium between Al_2Cu and Al_4Cu_9, it can be seen that the thermodynamics drive force for formation of AlCu was higher than those for the other phases (see the dash line in Fig. 5), which was in good agreement with the experimental observations [12, 15].

Kinetics of growth

As the layer thickness bears a direct relation with growth kinetics, the average thicknesses of the AlCu, Al_2Cu, and Al_4Cu_9 layers and the total intermetallic layer can be used to determine the kinetic parameters involved in the diffusion process. In general, the dependence of the thickness of an interdiffusion layer on diffusion time at a given temperature can be described by the following empirical relationship [30]:

$$w = kt^{n} \tag{7}$$

where w is the thickness of reaction layer, k the proportional factor, t the diffusion time, and n the time exponent. If a growth process is controlled by interfacial reaction at the growth site, linear growth behavior is expected and the time exponent will be 1 ($n = 1$). In contrast, parabolic growth implies that the kinetic is controlled by volume diffusion, i.e., $n = 0.5$. The layer thickness was plotted against $t^{1/2}$ and a linear regression fitting was performed, as shown in Fig. 6. It can be seen that linear regression analysis gave best-fit straight lines, and most of the linear correlation coefficient values (R^2) for these plots were higher than 0.96. The results indicated that the growth kinetics conformed well to the parabolic law, so the growth of intermetallic layers was volume diffusion-controlled in the temperature range studied.

For multi-phase diffusion couples, Wagner [30] presented a general approach where two types of rate constant, k^{I} and k^{II}, were proposed. The rate constant of the first kind, k_i^{I}, was introduced for the formation of phase i in a diffusion couple involving initially the pure components. The rate constant of the second kind, k_i^{II}, was introduced for formation of phase i ($i = 1,\ldots,n$) from phase $i - 1$ and $i + 1$. The k_i^{II} can be related to the intrinsic diffusion coefficients of the two components and further to the concentrations of defects and their diffusivities in phase i regardless of the characteristics of other phases. It was also recognized as the true rate constants or intrinsic rate constants by Garay et al. [31]. The relationship between k_i^{I} and k_i^{II} has been generalized by Buscaglia and Anselmi-Tamburini [32]:

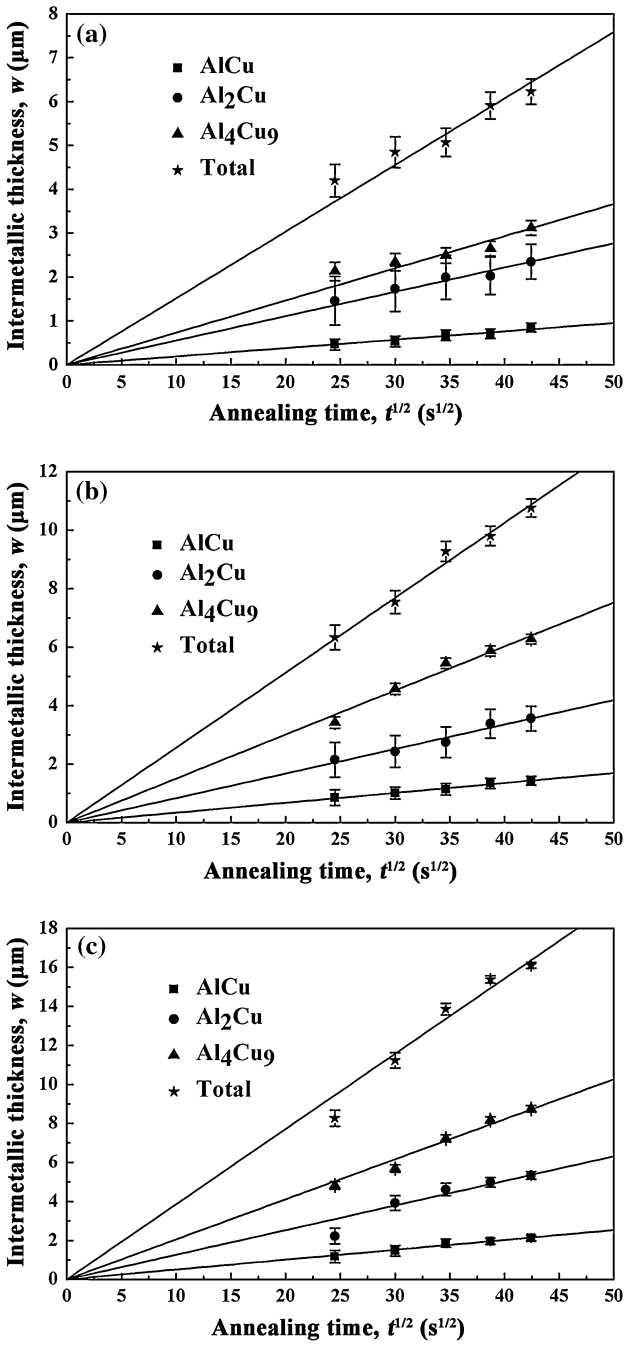

Fig. 6 Linear regression fit to the plot of the thickness of the intermetallic layers (w) versus the square root of time ($t^{1/2}$) for Cu–Al laminates annealed at **a** 673 K, **b** 723 K, and **c** 773 K. The error bars represent standard deviation

$$k_i^{II} = \frac{(v_{i-1} - v_{i+1})V_i}{(v_{i-1} - v_i)(v_i - v_{i+1})} C_i^2 \left[v_i \sum_{j=1}^{i-1} \frac{C_j}{V_j C_i} + \frac{v_i}{V_i} + \sum_{j=i+1}^{n} \frac{v_j C_j}{V_j C_i} \right] \quad i = 1, \ldots, n \tag{8}$$

where V_i is the molar volumes, v_i the stoichiometric coefficients of each phase normalized to one mol of component

Table 2 Calculated rate constants of the first kind for the intermetallic phases

Temperature (K)	k^{I}_{AlCu} (cm^2/s)	$k^{I}_{Al_2Cu}$ (cm^2/s)	$k^{I}_{Al_4Cu_9}$ (cm^2/s)	k^{I}_{Total} (cm^2/s)
673	3.63×10^{-12}	3.07×10^{-11}	5.37×10^{-11}	2.30×10^{-10}
723	1.15×10^{-11}	7.03×10^{-11}	2.26×10^{-10}	6.56×10^{-10}
773	2.56×10^{-11}	1.59×10^{-10}	4.21×10^{-10}	1.49×10^{-9}

Table 3 Calculated rate constants of the second kind for the intermetallic phases

Temperature (K)	k^{II}_{AlCu} (cm^2/s)	$k^{II}_{Al_2Cu}$ (cm^2/s)	$k^{II}_{Al_4Cu_9}$ (cm^2/s)
673	1.43×10^{-10}	7.15×10^{-11}	6.85×10^{-10}
723	4.11×10^{-10}	1.71×10^{-10}	2.35×10^{-9}
773	9.08×10^{-10}	3.80×10^{-10}	4.68×10^{-9}

B ($A_{v_i}B$), and $C_i = \sqrt{k_i^{I}}$. Here, the k_i^{I} equal to the calculated values of k_i^2 as listed in Table 2.

Values of k_i^{II} represent the intrinsic property of each phase, depending only on the interdiffusion coefficient and the free energy of formation of that phase. The values of k_i^{II} for the formed phases were calculated and reported in Table 3. The obtained results show that in the temperature range 673–773 K, the intrinsic rate constant of Al_4Cu_9 is higher than those of the other two phases.

The following simple Arrhenius-type relationship was used to determine the apparent activation energy for diffusion-controlled growth:

$$k^2 = k_0^2 \exp\left(\frac{-E_a}{RT}\right) \tag{9}$$

Or

$$\ln k^2 = \ln k_0^2 - \frac{E_a}{RT} \tag{10}$$

where k_0^2 is the frequency factor, E_a the apparent activation energy, R the gas constant (8.314 J/mol K), and T the absolute temperature. The activation energy can be obtained from plots of ln k^2 versus the reciprocal of temperature T, as shown in Fig. 7. The calculated apparent activation energies for the growth of AlCu, Al_2Cu, Al_4Cu_9, and the total intermetallic layer (AlCu + Al_2Cu + Al_4Cu_9) were 84.6 ± 5.3, 71.1 ± 2.6, 89.8 ± 6.9, and 80.8 ± 2.5 kJ/mol, respectively.

The apparent activation energies for the growth of Cu–Al intermetallic layers in the literatures and this study are summarized in Table 4. It can be seen that these values were scattered. The discrepancy among the activation energies can originate from the difference in the diffusion couple methods, aging conditions (temperature and time), and analytical method used [33]. The activation energies obtained in this study were lower than those in most of previous studies, except that of Braunović and Alexandrov [34], where an AC current was employed. Different from all the previous studies, in this study a DC current (≤200 A/cm^2) was used during the PAS process. The lower activation energies can result from the employing of the DC current, as argued by Garay et al. [31] that the DC current can enhance the growth of intermetallic phases and lower the related apparent activation energies in Ni–Ti system.

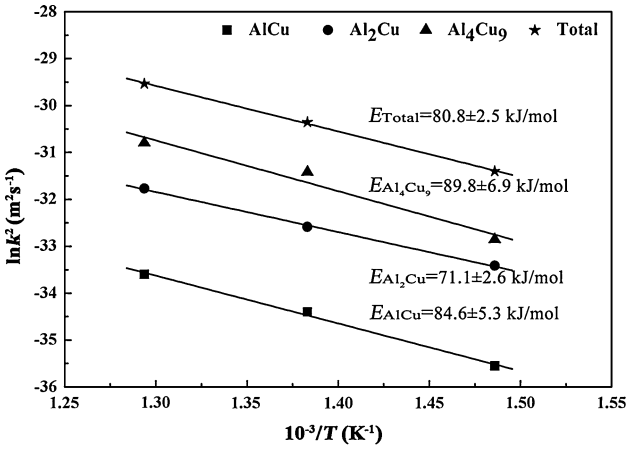

Fig. 7 An Arrhenius plot of the Al_4Cu_9, AlCu, Al_2Cu, and total intermetallic layer growth

Conclusions

The formation of intermetallic phases in diffusion-bonded multi-laminated Cu/Al couples has been investigated in the temperature range 673–773 K for 10–30 min. The main conclusions are summarized as follows:

(1) The interface in the diffusion-bonded Cu/Al laminates exhibits planar morphology, and three intermetallic phases, Al_4Cu_9, AlCu, and Al_2Cu, arrayed in sequence from Cu to Al, form at the interface. The effective heat of formation (EHF) model explains the appearance of Al_2Cu as the first phase in the diffusion zone. The formation of Al_4Cu_9 in preference to AlCu can be attributed to higher driving force for formation.

(2) The relationships between each layer thickness and reaction time follow the parabolic law, indicating that

Table 4 Values of the activation energy E_a obtained by several authors

Temperature range (K)	E_a (kJ/mol K)				Reference
	AlCu	Al_2Cu	Al_4Cu_9	Total	
673–808	82.0	122.6	132.2	–	Funamizu and Watanabe [6]
473–813	–	97.5	117.9	107.9	Chen and Hwang [15]
373–773	98.4	107.5	–	110.2	Lee et al. [10]
673–773	89.8	71.1	84.6	80.8	Present work

the growth kinetic of the intermetallic phases is diffusion-controlled.

(3) The temperature dependence of growth of the intermetallic layers conforms to an Arrhenius relation. The calculated activation energies for the growth of AlCu, Al_2Cu, Al_4Cu_9, and the total layer (AlCu + Al_2Cu + Al_4Cu_9) are 84.6 ± 5.3, 71.1 ± 2.6, 89.8 ± 6.9, and 80.8 ± 2.5 kJ/mol, respectively.

Acknowledgements This study is supported by the Natural Science Foundation of China (50972117, 51002114), and the postdoctorial Science Fundation of China (20100470089).

References

1. Wang CH, Chen SW (2008) Intermetallics 16:524
2. Heness G, Wuhrer R, Yeung WY (2008) Mater Sci Eng A 483:740
3. Hentzell HTG, Thompson RD, Tu KN (1983) J Appl Phys 54: 6923
4. Garcia VH, Mors PM, Scherer C (2000) Acta Mater 48:1201
5. Jiang HG, Dai JY, Tong HY, Ding BZ, Song QH, Hu ZQ (1993) J Appl Phys 74:6165
6. Funamizu Y, Watanabe K (1971) Trans Jpn Inst Met 12:147
7. Hannech EB, Lamoudi N, Benslim N, Makhloufi B (2003) Surf Rev Lett 10:677
8. Peng XK, Heness G, Yeung WY (1999) J Mater Sci 34:277. doi:10.1023/A:1004497304095
9. Abbasi M, Karimi Taheri A, Salehi MT (2001) J Alloys Compd 319:233
10. Lee WB, Bang KS, Jung SB (2005) J Alloys Compd 390:212
11. Yamazaki K, Risbud SH, Aoyama H, Shoda K (1996) J Mater Process Technol 56:955
12. Calvo FA, Ureng A, Gomez De Salazar JM, Molleda F (1988) J Mater Sci 23:2273. doi:10.1007/BF01115800
13. Hang CJ, Wang CQ, Mayer M, Tian YH, Zhou Y, Wang HH (2008) Microelectron Reliab 48:416
14. Murray JL (1985) Inst Met Rev 30:211
15. Chen C, Hwang W (2007) Mater Trans 48:1938
16. Nakamura M, Yonezawa Y, Nakanishi T, Kondo K (1977) WIRE J 10:71
17. Pretorius R, Vredenberg AM, Saris FW, de Reus R (1991) J Appl Phys 70:3636
18. Pretorius R, Marais TK, Theron CC (1993) Mater Sci Rep 10:1
19. Laik A, Bhanumurthy K, Kale GB (2004) Intermetallics 12:69
20. Xu L, Cui YY, Hao YL, Yang R (2006) Mater Sci Eng A 435–436:638
21. Zhang DL, Ying DY (2001) Mater Sci Eng A 301:90
22. Pan JS, Tong JM, Tian MB (1998) Foundations of materials science. Tsinghua University Press, Beijing
23. Miedema AR (1976) J Less-Common Met 46:67
24. Miedema AR, De Boer FR, Boom R (1977) Calphad 1:341
25. Miedema AR, De Châtel PF, De Boer FR (1980) Physica B 100:1
26. De Boer FR, Boom R, Mattens WCM, Miedema AR, Niessen AK (1988) Cohesion in metals: transition metal alloys. North-Holland, Amsterdam, Netherlands
27. Bakker H, Zhou GF, Yang H (1995) Prog Mater Sci 39:159
28. Barin I, Sauert F, Schultze-Rhonhof E, Wang S (1989) Thermochemical data of pure substances. VCH, New York
29. Zhang BW, Hu WY, Shu XL (2003) Theory of embedded atom method and its application to materials science-atomic scale materials design theory. Hunan University Publication Press, Changsha, China
30. Wagner C (1969) Acta Metall Mater 17:99
31. Garay JE, Anselmi-Tamburini U, Munir ZA (2003) Acta Mater 51:4487
32. Buscaglia V, Anselmi-Tamburini U (2002) Acta Mater 50:525
33. Kim DG, Jung SB (2005) J Alloys Compd 386:151
34. Braunović M, Alexandrov NA (1994) IEEE Trans Part A 17:261